Direct photoelectron-diffraction method for adsorbate structural determinations

V. Fritzsche*
Fritz-Haber-Institut der Max-Planck-Gesellschaft, Faradayweg 4-6, D W-1000 Berlin 33, Germany

D. P. Woodruff
Physics Department, University of Warwick, Coventry CV4 7AL, United Kingdom
(Received 23 July 1992)

A systematic search technique is proposed for low-energy photoelectron diffraction, which allows a direct determination of the bond axes from the emitter to the nearest backscatterers. It makes use of the fact that the Fourier transform of a photoelectron diffraction spectrum recorded in the scanned energy mode will show a maximum in the direction corresponding to a nearest-neighbor atom lying directly behind the emitter. The measurements are best performed with a large detector opening and a low energy resolution that allows short data accumulation times. Multiple-scattering calculations for a model system demonstrate that the position of the backscattering peak can be determined within an error of $\pm 3°$. This implies a spatial resolution perpendicular to the bond axis of about ± 0.1 Å, better than that achieved by holographic reconstruction techniques that use much larger amounts of experimental data.

I. INTRODUCTION

In the last decade photoelectron diffraction (PD) has been established as a useful technique for the determination of adsorption sites and bond lengths. In PD experiments the intensity of a photoelectron core-level peak from one of the adsorbate atoms is recorded as a function of the kinetic energy or as a function of the emission angle. In these spectra energy-dependent or angle-dependent intensity modulations are observed, which result from the interference between the direct wave coming from the excited atom and the scattered waves originating at the neighboring substrate and adsorbate atoms.

The main character of the structural information contained in the diffraction patterns depends essentially on the kinetic energy of the photoelectrons.

(i) At high photoelectron energies (typically between 400 and 1500 eV) the scattered waves show a dominant peak in the forward-scattering direction. Hence, the atoms lying above the emitter atom give rise to pronounced peaks in the angular distribution of the photoelectrons, from which the direction of major bond axes of the adsorbed molecules can be obtained rather directly.[1] Intermolecular forward-scattering directions can also be found in the angular map of the intensity, from which conclusions about the arrangement of molecules within the overlayer can be drawn.[2]

(ii) At low photoelectron energies (typically between 50 and 400 eV) backscattering processes at substrate atoms play an essential role and the PD spectra are mainly determined by the position of the emitter relative to the underlying substrate. In this energy range PD spectra have usually been measured in the scanned energy mode at a set of different emission angles. PD data collected under these conditions allow the adsorbate-substrate registry to be found; in particular, one can distinguish between different high-symmetry adsorption sites and can determine the distance between the emitter atom and the top layer of the substrate. The degree of relaxation between the upper substrate layers has also been explored successfully by this technique.[3]

An essential drawback of low-energy PD investigations, however, is that the desired structural information can be obtained from the PD spectra only by a trial and error procedure; extensive multiple-scattering calculations must be carried out for different possible structures and the results compared with the experimental data. Several of the structural parameters must then be varied until the best agreement between theory and experiment is found. This inefficient procedure, which is also used in conventional low-energy electron-diffraction (LEED) investigations, makes the structure determination cumbersome and tedious. Obviously, the difficulties of structural optimization [typically achieved with the help of some kind of objective reliability factor (R factor)] increase drastically with the number of free parameters in the model.

The development of direct methods for the analysis of electron-diffraction data is currently attracting considerable interest in surface physics.[4] Much of this work related to local diffraction techniques has been inspired by the paper of Szöke,[5] in which attention was drawn to the fact that familiar electron-diffraction patterns can be regarded as a natural extension of holographic microscopy. Barton[6] has shown that PD intensity distributions recorded at a fixed energy in a two-dimensional angle space can be inverted by a Fourier transform. The result should be a three-dimensional image of the local geometry around the emitter with atomic resolution. This holographic reconstruction method has been tested with computer-simulated photoelectron-diffraction data[6] and computer-simulated diffuse LEED patterns.[7]

So far these holographic reconstructions suffer from considerable problems.

(i) The fact that both the reference wave and the scattered waves are anisotropic spherical waves can lead to the images of the atoms being shifted considerably from their true positions.

(ii) The uncertainity principle implies restrictions on the resolution in the **r** space. In directions parallel to the surface a resolution of about 0.5 Å can be achieved, but the resolution perpendicular to the surface is more than four times poorer,[8] and the atomic images appear as elongated ellipsoidal blobs.

(iii) In addition to the well-known twin images, many other features are seen with significant magnitude in the Fourier transform which cannot be attributed to true atomic positions.

Although a number of more sophisticated reconstruction algorithms have since been developed,[9–12] the situation has not changed substantially in the low-energy region.[12,13] Holographic reconstructions of good quality have been obtained only at high energies in the forward-scattering geometry,[10,14,15] but in these situations the directions of bond axes can be obtained without holographic inversion from the forward-scattering peaks.

Recently, an alternative method for a quasidirect structure determination in the low-energy region has been proposed.[16] It is based on the observation that strong modulations in the energy-scan PD spectra often occur in directions for which a neighboring atom lies directly behind the emitter.[17] The essential idea is that at certain energies the effect of backscattering processes at the nearest-neighbor atoms can be easily detected in angular maps of the PD intensity. At energies where the condition for a constructive interference between the direct wave and the backscattered one is fulfilled, the photoemission intensity will show a peak in the direction of the bond axis and, conversely, at energies where the condition of a destructive interference is fulfilled, the photoelectron intensity has a minimum along the interatomic bond direction. These selected energies, at which the measurements have to be performed, can be calculated from a simple model if one has a reasonable estimate for the interatomic distance between the emitter and the backscatterer. On the basis of experimental data for Cu(110)-CO and Cu(110)(2×1)-O it was shown that such a real-space technique has a spatial resolution comparable to that of holographic inversion methods.[16]

In the present paper this idea will be extended towards a more systematic search method for the direction of the nearest backscatterers in real space, which does not rely on the prior estimate of the emitter-backscatterer distance.

II. THE "BACKSCATTERING EFFECT"

The PD intensity for a simple system consisting of an emitter (s core state) and one scattering atom is given in the single-scattering plane-wave approximation by

$$I(\mathbf{k}) \propto \left| \hat{\epsilon}\cdot\hat{\mathbf{k}} + \frac{\hat{\epsilon}\cdot\hat{\mathbf{R}}}{R} f(\hat{\mathbf{k}}\cdot\hat{\mathbf{R}}) \exp(ikR[1-\hat{\mathbf{k}}\cdot\hat{\mathbf{R}}]) \right|^2 , \quad (1)$$

where $\hat{\mathbf{R}}$ (unit vector) is the direction from the emitter to the scatterer, R the emitter-scatterer distance, $\hat{\mathbf{k}}$ the unit vector pointing towards the detector, $\hat{\epsilon}$ the polarization vector, and $k = \sqrt{2mE}/\hbar$ the wave number. The scattering amplitude $f(\cos\theta)$ is a complex function of the energy and the scattering angle $\cos\theta = \hat{\mathbf{k}}\cdot\hat{\mathbf{R}}$. The modulus of the scattering amplitude for a typical substrate atom is shown in Fig. 1. It has a large maximum in the forward-scattering direction ($\theta = 0°$). For low electron energies there exists an additional peak in the backscattering direction ($\theta = 180°$), which is strong enough to be seen in structure investigations. This secondary peak is larger than all other structures in the interval $30° \leq \theta \leq 180°$. The half width of this peak is about 30°.

However, there is an essential difference between the forward-scattering and backscattering regime, which arises from the phase factor in Eq. (1). In the forward-scattering direction we have $\hat{\mathbf{k}}\cdot\hat{\mathbf{R}} = 1$ and this phase factor is equal to one. Hence, the peak in the forward-scattering direction is present at each energy. In the backscattering geometry there is $\hat{\mathbf{k}}\cdot\hat{\mathbf{R}} = -1$, which means that the phase factor runs through all directions in the complex plane when the energy is varied. The intensity

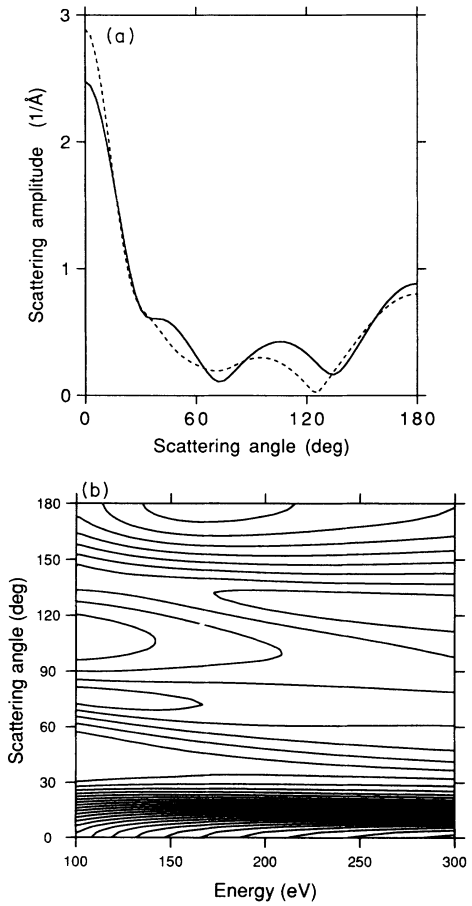

FIG. 1. Modulus of the scattering amplitude for Ni: (a) at $E = 150$ eV (solid line) and $E = 250$ eV (dashed line) and (b) as contour plot. The profiles shown in the panel (a) have been taken at lines of constant energy in panel (b).

dependence on energy thus shows maxima, minima, and various intermediate structures in the backscattering direction. In Fig. 2 this is illustrated using a system which contains an isotropic emitter (s-wave source) and a single scatterer. For a set of energies between 150 and 350 eV the normalized intensity $I(\theta)/I_0$, where I_0 is the isotropic intensity coming directly from the emitter, is shown in the backscattering region. The envelope of these curves is determined essentially by $|f(\cos\theta)|$. In order to find the true backscattering direction from $I(\hat{\mathbf{k}})$ one can choose a set of special energies,[16] if one has prior knowledge of the emitter-scatterer distance R (which would typically be achieved by using a reasonable estimate of its value).

This restriction, which certainly constrains the range of applicability of the method, can be overcome by measuring the PD intensity as a function of the energy and applying a Fourier transform to the modulation function $\chi(\mathbf{k})$,

$$u(\hat{\mathbf{k}},r)=\left|\int dk\,\chi(\mathbf{k})e^{-ikr}\right|. \tag{2}$$

$\chi(\mathbf{k})$ is obtained from the PD intensity $I(\mathbf{k})$ by removing the direct intensity contribution of the excited atom $I_0(\mathbf{k})$, which is a smooth function of both energy and emission direction,[3]

$$\chi(\mathbf{k})=\frac{I(\mathbf{k})-I_0(\mathbf{k})}{I_0(\mathbf{k})}. \tag{3}$$

For fixed directions $\hat{\mathbf{k}}$ the function $u(\hat{\mathbf{k}},r)$ has been intensely studied in angle-resolved photoemission fine-structure spectroscopy (ARPEFS) investigations,[3] which have shown that valuable conclusions on the adsorption site can be drawn from these Fourier spectra.

In the single-scattering picture underlying Eq. (1) it follows straightforwardly that the function $u(\hat{\mathbf{k}},r)$ will have a maximum in the backscattering direction $\hat{\mathbf{k}}=-\hat{\mathbf{R}}$ and at a distance r, which is roughly twice the bond length R (the difference being associated with the k dependence of the scattering amplitude). For finding the backscattering peak in the three-dimensional space $(\hat{\mathbf{k}},r)$ it is sufficient to determine for each direction $\hat{\mathbf{k}}$ the coordinate $r_{\max}(\hat{\mathbf{k}})$ where the maximum of $u(\hat{\mathbf{k}},r)$ occurs and to plot these maxima

$$U(\hat{\mathbf{k}})=\max_r u(\hat{\mathbf{k}},r) \tag{4}$$

as a function of the emission direction $\hat{\mathbf{k}}$, i.e., as function of the polar angle Θ and the azimuthal angle Φ.

The width of the backscattering peak in $U(\hat{\mathbf{k}})$ is mainly determined by the modulus of the scattering amplitude in the backscattering region. Furthermore, this peak shape can be influenced positively by a proper choice of the polarization vector. Ideally we use $\hat{\boldsymbol{\epsilon}}\|\hat{\mathbf{k}}$, in which case the first term in Eq. (1) will become one (constant contribution of the direct wave) and the factor in front of the scattering amplitude will be $\hat{\mathbf{k}}\cdot\hat{\mathbf{R}}=\cos\theta$, which has an extremum at the scattering angle $\theta=180°$ and thus supports the formation of the backscattering maximum in $u(\hat{\mathbf{k}},r)$. From Eq. (1) it follows that the magnitude of the peak in $U(\hat{\mathbf{k}})$ is proportional to R^{-1}. Hence the backscattering maximum in the Fourier spectrum is larger the smaller the distance between emitter and backscatterer is.

There exist two additional parameters, which can be optimized in the experiments: the energy resolution of the monochromator and electron-energy analyzer[18] and the angular resolution of the detector.[19,20] Including these effects and assuming $\hat{\boldsymbol{\epsilon}}\|\hat{\mathbf{k}}$, one obtains for the leading terms of the PD intensity considered in Eq. (1)

$$I(\mathbf{k})\propto 1+\frac{\cos\theta}{R}\,|f(\cos\theta)|\cos[kR(1-\cos\theta)+\psi(\theta)] \times a(\alpha kR\sin\theta)\,e^{-b(\Delta E\,R[1-\cos\theta])^2}, \tag{5}$$

where $\psi(\theta)$ is the phase of the scattering amplitude. The influence of a circular detector opening is described approximately by the aperture function $a(x)=(2/x)\,J_1(x)$, in which α is the half-angle of the conical aperture. This aperture function is shown in Fig. 3. The finite width of the energy distribution of the photoelectrons gives rise to an exponential damping term in Eq. (5), where ΔE is the half width at half maximum of the Gaussian distribution function assumed for the photoelectron energies, and $b=m(8\ln 2\,\hbar^2E)^{-1}$.

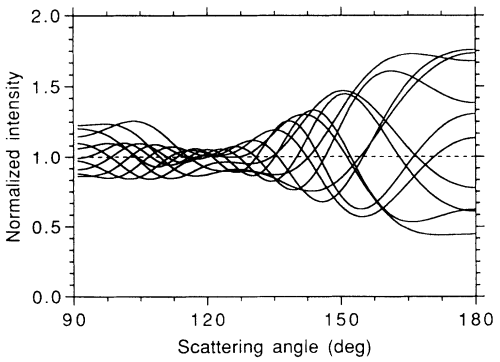

FIG. 2. Normalized PD intensity of a single Ni backscatterer as a function of the scattering angle θ for a set of equidistant wave numbers in the range 150–350 eV.

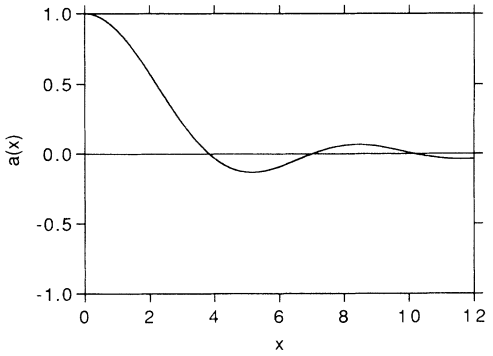

FIG. 3. Aperture function $a(x)=(2/x)\,J_1(x)$.

A systematic search for the nearest backscattering atoms can therefore be performed as follows: For a fixed direction $\hat{\mathbf{k}}$ the PD intensity is recorded as a function of the photoelectron energy, and thus of the wave number k. From these data the Fourier transform $U(\hat{\mathbf{k}})$ is calculated immediately. The measurements are then repeated for other directions $\hat{\mathbf{k}}$ in order to find the maxima in $U(\hat{\mathbf{k}})$, which give directly the bond axes from the nearest backscatterers to the emitter.

An important point is that these experiments can be carried out with unusually large values for the detector opening α and the width of the energy distribution ΔE. Because the intrinsic width of the backscattering peak in the scattering amplitude (Fig. 1) is large, our calculations show that a value of about 20° can be used for α. Such a large detector opening will give a high counting rate (this rate scales as α^2), so it should be possible to use a very short accumulation time for the data points. Moreover, the large detector angle improves the shape of the backscattering peak in $U(\hat{\mathbf{k}})$, since the aperture function $a\,(\alpha kR\sin\theta)$ in Eq. (5) [which has its maxima at $\theta = 0°$ and 180° (see Fig. 3)] further reduces the intensity for all positions of the scattering atom which do not lie exactly in the backscattering direction. This damping is greatest for scatterers far from the ideal backscattering and forward-scattering axis. In particular, the structures which occur in $|f(\theta)|$ around $\theta = 100°$ are weakened considerably by an α value of about 20°. A large energy spread ΔE smoothes the fine structures in the energy-dependent function $I(\mathbf{k})$ considered at a fixed direction $\hat{\mathbf{k}}$. The long period oscillations in the energy scans, however, which arise from single scattering at nearest neighbors remain largely unchanged. More quantitatively, this can be seen from the term $e^{-b(\Delta E\,R[1-\cos\theta])^2}$ in Eq. (5). If ΔE is about 10 eV, the resulting damping will be negligible for the single-scattering processes from the nearest backscatterers, but the contributions from many of the longer scattering pathways, and in particular from higher-order scattering pathways, will be weakened considerably. Of course, a large energy width of the electron distribution will also speed up the experiments provided the signal-to-background ratio remains satisfactory, since it increases the counting rate and reduces the number of energies which need to be measured as a coarser grid on the energy scale can be used.

III. MULTIPLE-SCATTERING CALCULATIONS

A key question in establishing the applicability of this idea is whether the backscattering intensity contribution from a single nearest-neighbor atom is sufficiently large relative to the scattering contributions from the large number of other atoms in the system. To investigate this problem we have performed numerical calculations for realistic systems to establish whether the "backscattering effect," which we want to use for a real-space structure determination, remains detectable after the superimposition of all the other scattered waves. As an example we present multiple-scattering calculations for the system Ni(111)-NH_3, which was recently investigated by energy-scan photoelectron diffraction.[21] The spherical-wave computations have been performed in the framework of a magnetic-quantum-number expansion by means of exact recursion formulas.[20] Scattering processes up to fourth order were included in these calculations. The scattering events at the hydrogen atoms have been neglected, since the scattering cross section of hydrogen is much smaller than that of the nickel atoms due to the large difference in the atomic numbers. The values for the inelastic mean free path of the electrons have been taken from Seah and Dench.[22] The sample temperature was assumed to be 100 K and the thermal vibrations of the nickel atoms were taken into account by means of temperature-dependent complex scattering phase shifts.[23] The intensity $I(\mathbf{k})$ was calculated in the energy range from 100 up to 350 eV, used in the previous experiments[21] on this system which led to the original structure determination. The resolution parameters used in the calculations presented here are $\alpha = 20°$ and $\Delta E = 10$ eV. The integration over the detector opening has been performed numerically, since the approximate aperture function $a(x)$ given above may not be accurate enough at such a large value of α.

In Figs. 4–6 the calculated values $U(\hat{\mathbf{k}})$ and $r_{\max}(\hat{\mathbf{k}})$ are presented as functions of the polar angle Θ (measured from the surface normal) for different adsorbate positions and for several azimuths which are defined in Fig. 7. The polarization vector of the photons has been assumed to be parallel to the emission direction. Obviously, when probing the PD intensity in the vicinity of the surface

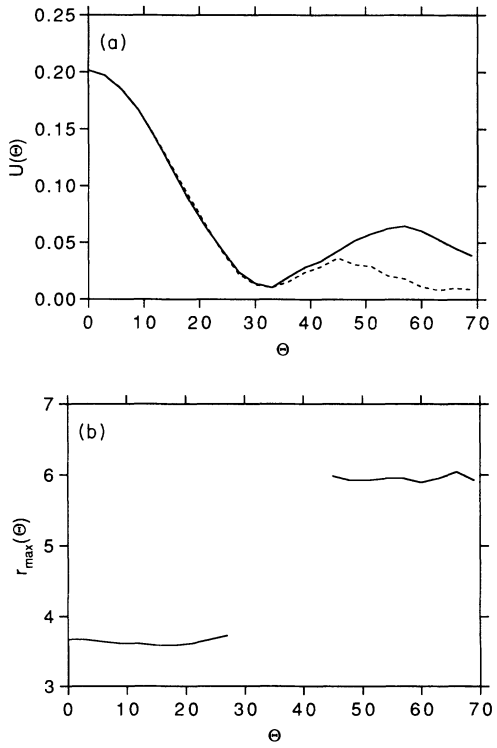

FIG. 4. Maxima in the Fourier transform of the energy-scan PD spectra from the atop site: $\Phi = 0°$ (solid line), $\Phi = 30°$ (dashed line).

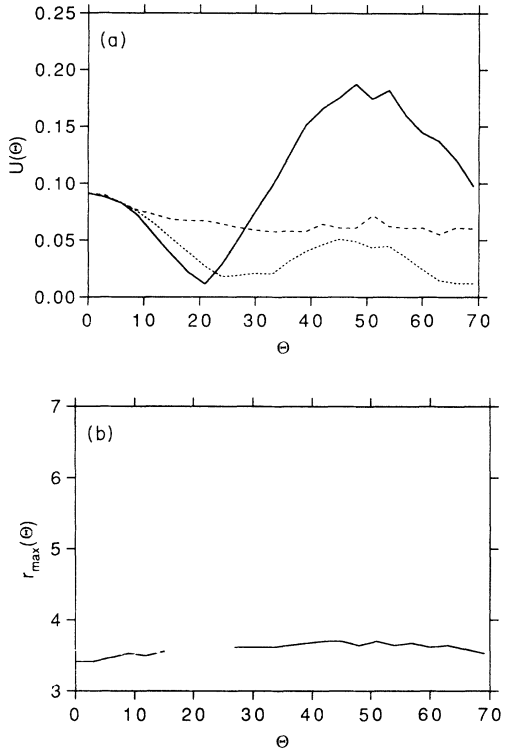

FIG. 5. Maxima in the Fourier transform of the energy-scan PD spectra from the fcc hollow site: $\Phi = 90°$ (solid line), $\Phi = 30°$ (long-dashed line), $\Phi = 0°$ (short-dashed line).

normal, this condition can be fulfilled only approximately in the experiment. The bond length between nitrogen and the nearest nickel neighbors was fixed at 1.97 Å, the value which was obtained in the PD investigations.[21]

If the nitrogen atom occupies an atop site, the function $U(\hat{\mathbf{k}})$ has a strong peak in the normal-emission direction [panel (a) of Fig. 4], which is clearly consistent with the fact that a backscattering nickel atom is directly below the emitter atom. The second maximum, which appears at $\Theta = 57°$ in the $\Phi = 0°$ azimuth, comes from one of the next-nearest-neighbor atoms in the top layer. The pure geometrical angle of this interatomic axis in the structure is $\Theta = 51.6°$, which will be shifted by refraction effects at the surface to a value of $\Theta = 54.2°$. In panel (b) of Fig. 4 it can be seen that the values for r_{max} are smaller than $2R = 3.94$ Å for the nearest neighbor at $\Theta = 0°$ and $2R = 6.35$ Å for the next-nearest neighbor at $\Theta = 57°$. Assuming that the energy dependence of $f(\cos\theta)$ is weak, it follows from Eq. (5) that for a vanishing detector opening ($\alpha = 0°$) and $\Delta E = 0$ eV the ridge of the backscattering peak in $u(\hat{\mathbf{k}}, r)$ should appear at $r_{max}(\theta) = R(1 - \cos\theta)$ having the maximum at $r_{max} = 2R$ and $\theta = 180°$, where R is the emitter–backscatterer distance and θ the scattering angle. Obviously, an integration over θ then has the consequence that in spectra obtained with a large α the peak position is shifted systematically to lower values of r, as it can be observed for the atop position in Fig. 4, where 30% of the shift in r_{max} is due to the large detector opening and 70 % due to the energy dependence of the scattering properties.

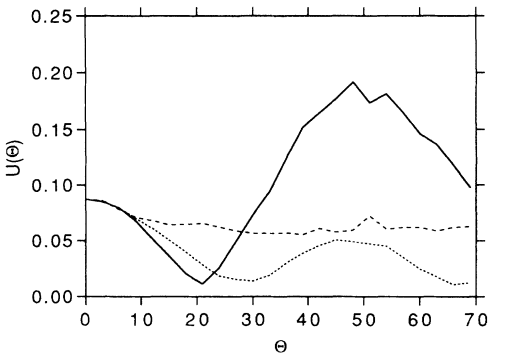

FIG. 6. Maxima in the Fourier transform of the energy-scan PD spectra from the hcp hollow site: $\Phi = 30°$ (solid line), $\Phi = 90°$ (long-dashed line), $\Phi = 0°$ (short-dashed line).

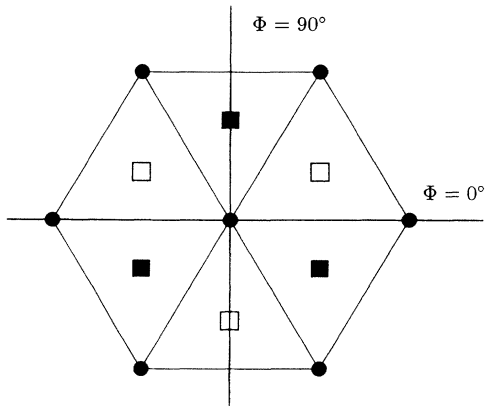

FIG. 7. High-symmetry adsorption sites on a Ni(111) surface: The substrate atoms are depicted as filled circles (first layer), empty boxes (second layer), and filled boxes (third layer). The considered adsorption sites are located directly above these atoms. Hence, the atop site is indicated by a filled circle, the fcc hollow site by a filled box and the hcp hollow site by an empty box.

It should be noted that in particular one of the higher-order scattering contributions has a noticeable influence on the backscattering effect. This is the double-scattering process which contains the emitting atom as a forward scatterer after the first backscattering process. In the ideal backscattering geometry it has the same path-length difference to the direct wave as the single backscattering process itself and, hence it contributes to the same peak in the Fourier spectrum. In Fig. 4 [panel (a)] about 5% of the peak height in normal-emission direction are caused by this double-scattering pathway.

In Fig. 5 the function $U(\hat{\mathbf{k}})$ is shown for the threefold hollow site on the Ni(111) surface which has the next atom directly below the adsorption place in the third layer of the substrate (fcc hollow site). The main peak from the nearest backscatterer can be seen around $\Theta = 48°$ in the $\Phi = 90°$ azimuth. The true polar angle of this bond axis is $\Theta = 46.8°$, which will be shifted in

the PD spectra due to the refraction at the surface potential towards 49°. An additional peak which cannot be attributed to a backscattering atom appears in normal-emission direction. It arises from a superposition of the tails of the three nearest-neighbor backscattering peaks. Hence, it can be considered to be more or less a result of the high symmetry of this direction. In agreement with this interpretation the value of r_{max} is about 3.4 Å for this secondary peak, which is smaller than $r_{max} = 3.7$ Å obtained for the main peaks in Figs. 4 and 5.

Furthermore, in Fig. 6 the function $U(\hat{\mathbf{k}})$ is shown for the other threefold coordinated adsorption site, the hcp hollow site, for which the next atom directly below the adsorption place occurs in the second substrate layer. These spectra look very similar to that of the fcc hollow site apart from an azimuthal rotation of 60° to realign the (top layer) nearest neighbors. This means that the structure differences in the second layer are completely dominated by the strong backscattering contributions from the nearest neighbors. Weak features associated with the atom in the second Ni layer can be seen only in the full Fourier transform $u(\hat{\mathbf{k}}, r)$ of the PD spectra around $r = 6.3$ Å in the normal-emission direction. However, these contributions are damped considerably due to the large value of ΔE.

It should be noted that the backscattering effect shows a considerable temperature dependence due to the strong influence of thermal vibrations on the Debye-Waller factor in backscattering geometry. All results shown so far have been obtained assuming isotropic harmonic vibrations of the atoms with amplitudes corresponding to a temperature of about 100 K, which can be realized experimentally by cooling with liquid nitrogen. In Fig. 8 it is shown how the structures in $U(\hat{\mathbf{k}})$ are weakened by increasing the temperature to 300 K.

In comparison with the sharp forward-scattering peaks, which are used for the structure investigations in the high-energy region,[1,2] the backscattering peaks in the Fourier transform $U(\hat{\mathbf{k}})$ shown in Figs. 4–6 are weaker and broader. However, the high-energy forward-scattering method is of limited value in the investigation of adsorption structures because the adsorbate typically lies *above* the substrate atoms, which then cannot forward scatter the adsorbate photoemitted electrons into the detector. Investigating substrate atom photoemission is also of little general use because the component of emission arising from the top-layer atoms cannot normally be distinguished from that of the underlying substrate. By contrast, low-energy photoelectron backscattering of the adsorbate photoemission is, as we have shown, a viable route to the determination of adsorbate-substrate registry.

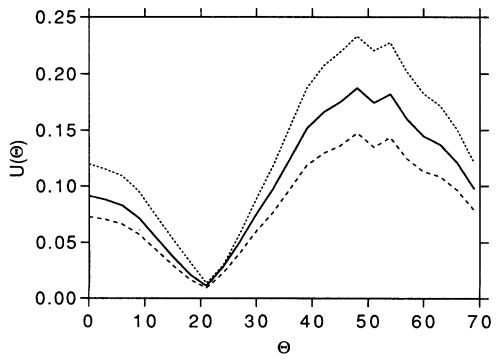

FIG. 8. Maxima in the Fourier transform of the energy-scan PD spectra from the fcc hollow site ($\Phi = 90°$): $T = 100$ K (solid line), $T = 300$ K (long-dashed line), and neglecting all vibrations (short-dashed line).

Although the half width of the backscattering maximum in $U(\hat{\mathbf{k}})$ (Figs. 4–6) is about 30°, the position of these peaks can be determined with an accuracy of ±3°, or better. For a bond length of 2 Å, as considered here, this means that the error in position perpendicular to the bond axis is ±0.1 Å, which is much better than the accuracy of holographic reconstructions. However, the bond length between the emitter and backscatterer should not be determined from measurements with such a large detector opening of $\alpha = 20°$, since under these conditions r_{max} is shifted systematically towards lower values as discussed above. Hence, in order to determine the bond length between the emitter and backscatterer more precisely one should perform an additional measurement with a higher angular and energy resolution for the backscattering direction in the scanned energy mode.

IV. CONCLUSIONS

The results of model calculations presented here demonstrate that the "backscattering effect," which occurs in the scattering amplitude for energies between 100 and 300 eV, can be utilized successfully for direct structure investigations. By exciting an s core level of an adsorbate atom it should be possible to determine the direction in which the nearest backscatterer in the underlying substrate is located with an accuracy of about ±3°. The proposed procedure requires the measurement of PD spectra in the scanned energy mode over an energy range of about 250 eV with a step width of 10 eV (i.e., 26 data points). In order to find the maxima in the Fourier transform $U(\hat{\mathbf{k}})$ these PD spectra have to be recorded on an angular mesh covering the whole two-dimensional angle space above the surface. These measurements are best performed with a large detector acceptance angle, which has the added benefit of making the data collection time short. Having used these data to identify the nearest-neighbor backscattering directions, we then propose that energy-scan PD spectra can be measured with a higher angular and energy resolution in these directions in order to determine the bond length between the emitter and backscatterer as accurately as possible.

Our method makes use of PD data $I(\mathbf{k})$ from a three-dimensional space (energy, polar angle, and azimuthal angle) similar to the sophisticated holographic reconstruction methods.[9–12] In contrast to these holographic methods which require amassing a huge amount of data in the two-dimensional angular space, we propose to filter out only that information which is relevant for finding

the nearest backscatterers. This can be done by using a large detector opening, which means that the PD intensity is probed by wide overlapping cones. Hence, the data recording is much faster in the proposed technique than in comparable holographic techniques. Notice that we have also assumed a fixed angle between the detector and the photon polarization vector, so the experiment can be performed by simply "rocking" the sample. Our method provides a rapid route to a first-order structure determination, which if neccessary can then be refined further by a full comparison of theoretical and experimental PD intensity data, which makes use of all the fine structure, measured in three-dimensional **k** space.

ACKNOWLEDGMENT

One of the authors (V.F.) would like to thank Professor A. M. Bradshaw for the support and the hospitality at the Fritz-Haber-Institut.

*Present address: Blackett Laboratory, Department of Physics, Imperial College of Science, Technology and Medicine, Prince Consort Road, London SW7 2BZ, United Kingdom. Permanent address: Institut für Theoretische Physik, Technische Universität Dresden, Mommsenstrasse 13, D O-8027 Dresden, Germany.

[1]L.-G. Petersson, S. Kono, N. F. T. Hall, C. S. Fadley, and J. B. Pendry, Phys. Rev. Lett. **42**, 1545 (1979); P. J. Orders, S. Kono, C. S. Fadley, R. Trehan, and J. T. Lloyd, Surf. Sci. **119**, 371 (1982); W. F. Egelhoff, Jr., *ibid.* **141**, L324 (1984); E. Holub-Krappe, K. C. Prince, K. Horn, and D. P. Woodruff, *ibid.* **173**, 176 (1986); D. A. Wesner, F. P. Coenen, and H. P. Bonzel, J. Vac. Sci. Technol. A **5**, 927 (1987); Phys. Rev. Lett. **60**, 1045 (1988); Phys. Rev. B **39**, 10 770 (1989); R. S. Saiki, G. S. Herman, M. Yamada, J. Osterwalder, and C. S. Fadley, Phys. Rev. Lett. **63**, 283 (1989).

[2]O. Knauff, U. Grosche, H. P. Bonzel, and V. Fritzsche, Mol. Phys. **76**, 787 (1992).

[3]S. W. Robey, J. J. Barton, C. C. Bahr, G. Lui, and D. A. Shirley, Phys. Rev. B **35**, 1108 (1987); C. C. Bahr, J. J. Barton, Z. Hussain, S. W. Robey, J. G. Tobin, and D. A. Shirley, *ibid.* **35**, 3773 (1987); S. W. Robey, C. C. Bahr, Z. Hussain, J. J. Barton, K. T. Leung, Ji-ren Lou, A. E. Schach von Wittenau, and D. A. Shirley, *ibid.* **35**, 5657 (1987); L. J. Terminello, X. S. Zhang, Z. Q. Huang, S. Kim, A. E. Schach von Wittenau, K. T. Leung, and D. A. Shirley, *ibid.* **38**, 3879 (1988); X. S. Zhang, L. J. Terminello, S. Kim, Z. Q. Huang, A. E. Schach von Wittenau, and D. A. Shirley, J. Chem. Phys. **89**, 6538 (1988); Li-Quiong Wang, A. E. Schach von Wittenau, Z. G. Ji, L. S. Wang, Z. Q. Huang, and D. A. Shirley, Phys. Rev. B **44**, 1292 (1991); Li-Quiong Wang, Z. Hussain, Z. Q. Huang, A. E. Schach von Wittenau, D. W. Lindle, and D. A. Shirley, *ibid.* **44**, 13 711 (1991).

[4]J. B. Pendry and K. Heinz, Surf. Sci. **230**, 137 (1990).

[5]A. Szöke, in *Short Wavelength Coherent Radiation: Generation and Applications*, edited by D. T. Attwood and J. Boker, AIP Conf. Proc. No. 147 (American Institute of Physics, New York, 1986).

[6]J. J. Barton, Phys. Rev. Lett. **61**, 1356 (1988).

[7]D. K. Saldin and P. L. de Andres, Phys. Rev. Lett. **64**, 1270 (1990).

[8]J. J. Barton, J. Electron Spectrosc. **51**, 37 (1990).

[9]S. Y. Tong, C. M. Wei, T. C. Zhao, H. Huang, and Hua Li, Phys. Rev. Lett. **66**, 60 (1991).

[10]S. Hardcastle, Z.-L. Han, G. R. Harp, J. Zhang, B. L. Chen, D. K. Saldin, and B. P. Tonner, Surf. Sci. **245**, L190 (1991); B. P. Tonner, Zhi-Lan Han, G. R. Harp, and D. K. Saldin, Phys. Rev. B **43**, 14 423 (1991); D. K. Saldin, G. R. Harp, B. L. Chen, and B. P. Tonner, *ibid.* **44**, 2480 (1991).

[11]S. Y. Tong, Hua Li, and H. Huang, Phys. Rev. Lett. **67**, 3102 (1991); H. Huang, Hua Li, and S. Y. Tong, Phys. Rev. B **44**, 3240 (1991).

[12]J. J. Barton, Phys. Rev. Lett. **67**, 3106 (1991).

[13]Peijun Hu and D. A. King, Nature **353**, 831 (1991).

[14]G. R. Harp, D. K. Saldin, and B. P. Tonner, Phys. Rev. Lett. **65**, 1012 (1990).

[15]G. R. Harp, D. K. Saldin, and B. P. Tonner, Phys. Rev. B **42**, 9199 (1990).

[16]R. Dippel, D. P. Woodruff, X.-M. Hu, M. C. Asensio, A. W. Robinson, K.-M. Schindler, K.-U. Weiss, P. Gardner, and A. M. Bradshaw, Phys. Rev. Lett. **68**, 1543 (1992).

[17]D. P. Woodruff, C. F. McConville, A. L. D. Kilcoyne, Th. Lindner, J. Somers, M. Surman, G. Paolucci, and A. M. Bradshaw, Surf. Sci. **201**, 228 (1988); Th. Lindner, J. Somers, A. M. Bradshaw, A. L. D. Kilcoyne, and D. P. Woodruff, *ibid.* **203**, 333 (1988); A. L. D. Kilcoyne, D. P. Woodruff, Th. Lindner, J. Somers, and A. M. Bradshaw, J. Vac. Sci. Technol. A **7**, 1926 (1989); A. W. Robinson, J. S. Somers, D. E. Ricken, A. M. Bradshaw, A. L. D. Kilcoyne, and D. P. Woodruff, Surf. Sci. **227**, 237 (1990); M. C. Asensio, M. J. Ashwin, A. L. D. Kilcoyne, D. P. Woodruff, A. W. Robinson, Th. Lindner, J. S. Somers, D. E. Ricken, and A. M. Bradshaw, *ibid.* **236**, 1 (1990); A. L. D. Kilcoyne, D. P. Woodruff, A. W. Robinson, Th. Lindner, J. S. Somers, and A. M Bradshaw, *ibid.* **253**, 107 (1991).

[18]V. Fritzsche, Surf. Sci. **265**, 187 (1992).

[19]J. J. Barton, S. W. Robey, and D. A. Shirley, Phys. Rev. B **34**, 778 (1986).

[20]V. Fritzsche, J. Phys. Condens. Matter **2**, 9735 (1990).

[21]K.-M. Schindler, V. Fritzsche, M. C. Asensio, P. Gardner, D. E. Ricken, A. W. Robinson, A. M. Bradshaw, D. P. Woodruff, J. C. Conesa, and A. R. González-Elipe, Phys. Rev. B **46**, 4836 (1992).

[22]M. P. Seah and W. A. Dench, Surf. Interf. Anal. **1**, 2 (1979).

[23]J. B. Pendry, *Low Energy Electron Diffraction* (Academic, London, 1974).

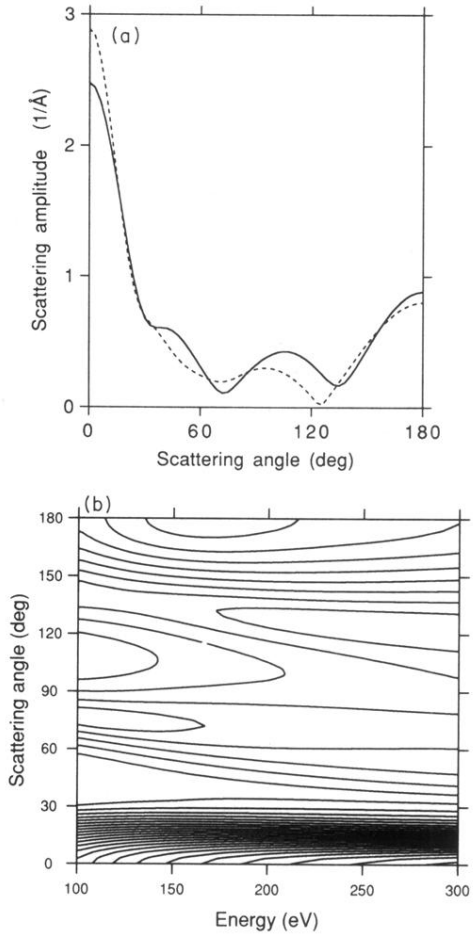

FIG. 1. Modulus of the scattering amplitude for Ni: (a) at $E = 150$ eV (solid line) and $E = 250$ eV (dashed line) and (b) as contour plot. The profiles shown in the panel (a) have been taken at lines of constant energy in panel (b).